Calculation of the Velocity and Shape of an Explosively Formed Projectile (EFP) Using Axisymmetric ALE

John Puryear[a], Ben Harrison[b], Lynsey Reese[c], Michael Oesterle[d]

[a]*ABS Group, 140 Heimer Rd. Suite 300, San Antonio, TX*

[b]*ABS Group, 140 Heimer Rd. Suite 300, San Antonio, TX*

[c]*NAVFAC Engineering and Expeditionary Warfare Center, Port Hueneme, CA*

[d]*NAVFAC Engineering and Expeditionary Warfare Center, Port Hueneme, CA*

Abstract

The symmetry common to most explosively formed projectiles (EFPs) permits their characterization using 2D axisymmetric analysis. Formation of an EFP entails volumetric expansion of the explosive and extensive plastic flow of the metal plate, both of which can be calculated using an Arbitrary Lagrangian Eulerian (ALE) method. Accordingly, the 2D axisymmetric ALE capability in LS-DYNA® was applied to calculate the velocity and shape of an EFP. The methodology was validated against EFP velocity and shape measurements published in SAND-92-1879 by Hertel.

**MAT_HIGH_EXPLOSIVE_BURN and Jones-Wilkins-Lee (JWL) equation of state (EOS) were used for the LX-14 high explosive backing the copper plate. The copper plate and steel casing were included using *MAT_JOHNSON_COOK and *EOS_GRUNEISEN. The calculated peak velocity of the EFP was in excellent agreement with the peak velocity published by Hertel. However, the calculated shape did not agree with the experimental shadowgraph of the plate. Specifically, the calculated shape was elongated compared to the measurement and continued to elongate as long as the calculation was continued. In other words, the shape of the copper plate did not reach a dynamic equilibrium. This result for the shape was inconsistent with a result published by Van Dorsselaer and Lapoujade, who found close agreement between his calculated shape and Hertel's measured shape.*

In this paper, the methodology for calculating the EFP peak velocity and shape is described. The calculated results are compared to measurements from Hertel. Finally, possible sources for the inaccuracy of the calculated shape are investigated. These include the element size and formulation, initial geometry of EFP, explosive equation of state and the constitutive model for the copper plate.

Introduction

The symmetry common to most explosively formed projectiles (EFPs) permits their characterization using 2D axisymmetric analysis. Formation of an EFP entails volumetric expansion of the explosive and extensive plastic flow of the metal plate, both of which can be calculated using an Arbitrary Lagrangian Eulerian (ALE) finite element method. Accordingly, the 2D axisymmetric ALE capability in LS-DYNA was applied to calculate the velocity and shape of an EFP. The methodology was validated against EFP velocity and shape measurements published by Hertel [1].

The calculated peak velocity of the EFP was in excellent agreement with the peak velocity published by Hertel. However, the calculated EFP shape did not agree with the experimental shadowgraph. Specifically, the calculated shape was elongated compared to the measurement and continued to elongate as long as the calculation was continued. This result for the shape was inconsistent with a result published by Van Dorsselaer and Lapoujade, who found close agreement between their calculated shape and Hertel's measured shape.

In this paper, the methodology for calculating the EFP peak velocity and shape is described. The calculated results are compared to measurements from Hertel. Finally, possible sources for the inaccuracy of the calculated

shape are discussed. These include the element size and formulation, initial geometry of EFP, explosive equation of state and the constitutive model for the copper plate.

Validation Data and Geometry

Hertel reports an initial velocity and shape for an explosively-backed copper flyer plate, as detailed in SAND-92-1879 [1]. The plate is an OFHC (oxygen-free high thermal conductivity) copper explosive lens propelled by the high explosive LX-14. The casing is AISI 4340 steel. Additional details and the cross section of the assembly are provided in Hertel [1].

ALE Controls and Domain

The axisymmetric Eulerian domain was composed of 2D shell elements with the section shown in Table 1. The domain itself is shown in Figure 1. The domain element size was 0.7mm. *INITIAL_VOLUME_FRACTION_GEOMETRY was used to define the parts. The domain was first filled with air. Beam elements were used to define the fill volumes for the explosive, casing and flyer plate, each of which was sequentially filled. It is noted that the normals of the beam elements must all point either into the region defining the cross section or all out of that region for the fill the be successful.

Table 1. Eulerian Domain – Section Definition

Keyword	aleform	elform
*SECTION_ALE2D	11	14

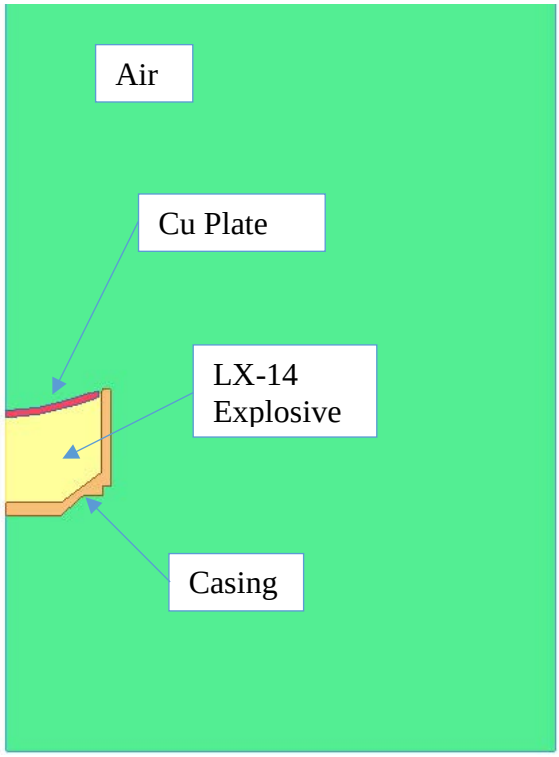

Figure 1. Hertel Validation - Eulerian Domain with Filled Parts

Constitutive Model

The parts of the axisymmetric model, their constitutive models, and sources of material inputs are summarized in Table 2. The Johnson-Cook damage and fracture model that is included in implementation of *MAT_015 was used for characterizing damage to the flyer plate and casing material.

Table 2. Constitutive Model by Part

Part	Material	No.	Keyword	Input Data Source(s)
Flyer plate	OFHC Copper	015	*MAT_JOHNSON_COOK	Johnson and Cook [2], [3]
Casing	4340 Steel	015	*MAT_JOHNSON_COOK	
Explosive	LX-14	008	*MAT_HIGH_EXPLOSIVE_BURN	Hertel [1], LS-DYNA Keyword User's Manual [4]
Air	Air at STP	009	*MAT_NULL	

Equation of State

The parts of the axisymmetric model, their equations of state, and sources of equation of state (EOS) inputs are summarized in Table 3.

Table 3. Equations of State by Part

Part	Material	No.	Keyword	Input Data Source(s)
Flyer plate	OFHC Copper	004	*EOS_Gruneisen	Steinberg [5]
Casing	4340 Steel	004	*EOS_Gruneisen	
Explosive	LX-14	002	*EOS_JWL	Hertel [1]
		014	*EOS_JWLB	LS-DYNA Keyword User's Manual [4]
Air	Air at STP	001	*EOS_LINEAR_POLYNOMIAL	Otsuka [6]

Use of the JWL EOS was the starting point for the explosive. Hertel [1] reports JWL constants for the LX-14, and JWL is established for calculating explosive expansion. The caution in using JWL is the engineering simplifications that it employs. For example, Fuller et al. at the University of Sheffield [7] report that the JWL EOS may over-predict peak pressures and impulses for close-in detonation. Fuller et al. indicate that the assumption of near instantaneous energy release from detonation may cause this over-prediction.

Given these cautions, alternatives to the JWL EOS were considered. These included JWLB (Jones-Wilkins-Lee-Baker), IGNIITION_AND_GROWTH_OF_REACTION_IN_HE and JWL_AFTERBURN. JWLB was particularly promising because it is a form of the JWL developed by Baker et al. [8] specifically for EFPs and shaped charges. The JWLB form is intended to refine the assumption of a uniformly expanding cylinder to calculate the Jones-Wilkins-Lee (JWL) constants.

Assumption of a uniformly expanding cylinder does not account for all the work done on the cylinder by the explosive. Specifically, some of the work done by explosive products (axial flow of cylinder, bending of cylinder, etc.) is not included in the Gurney energy/volume, a parameter critical to EFP calculations. The implication is that the explosive can do more work than the JWL constants predict. Accordingly, explosives tests would be expected to produce a higher velocity than calculated using the JWL EOS.

The input constants of LX-14 are available for JWLB; in fact, these are included in LS-DYNA Keyword User's Manual [4]. LX-14 inputs for IGNIITION_AND_GROWTH_OF_REACTION_IN_HE and JWL_AFTERBURN could not be obtained. Those for IGNITION_AND_GROWTH_OF_REACTION_IN_HE are forthcoming from work by Tarver but were not available at this time of this study [9].

Calculation Results – Peak Velocity

As noted above, the outputs of interest from the calculation were the peak velocity and shape of the EFP. The calculated peak velocity was in good agreement with the velocity measured in the experiment. Hertel reports a peak velocity of 0.228 cm/usec. The peak velocity in the calculation (at ~100 usec) using JWLB was 0.228 cm/usec, whereas it was 0.225 using JWL. These results are compared in Table 4 and illustrated in Figure 2. The calculated velocities in Figure 2 are rigid-body velocities of the EFP along the axis of symmetry.

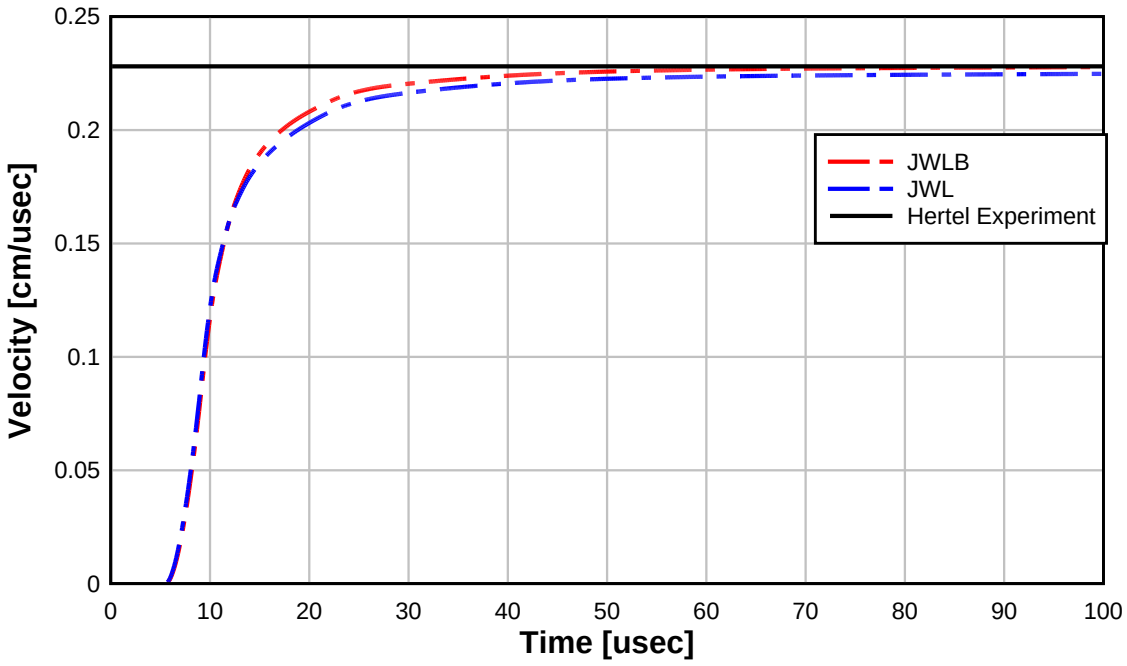

Figure 2. Peak Velocity – JWLB and JWL EOS vs. Experiment

Table 4. Peak Velocity – Calculation vs. Experiment

Case	Plate Peak Velocity [cm/usec]	% Difference vs. Experiment
Experiment	0.228	-
Calculation - JWLB	0.228	0.00%
Calculation - JWL	0.225	1.32%

The results summarized in Table 4 are consistent with the development of the JWLB EOS. Specifically, JWLB was intended as a refinement of the JWL EOS that applies all the explosive energy to the plate in contact. The JWLB EOS results in a slightly higher peak velocity compared to JWL.

Less clear is how these results relate to work by Fuller et al. Their finding that the JWL EOS may over-predict peak pressures and impulses for close-in detonation would suggest over-prediction of peak velocity in a case like the Hertel experiment. However, the JWL peak velocity was below the measured velocity. Of course, a close-in detonation does not act on a target identically to how explosive in contact with a plate acts on it, but it is unclear how over-prediction in the close-in detonation case can coexist with a slight under-prediction in the EFP velocity.

Calculation Results – EFP Shape

Van Dorsselaer and Lapoujade's reported EFP shape is shown next to the shapes calculated with JWLB and JWL, respectively, in Figure 3, and the dimensions of the calculated and measured EFP shapes are listed in Table 5. These are the EFP shapes at the peak velocity.

The basic observation is that the EFP shapes presently calculated by LS-DYNA are less compact than the measured shape and the shape reported by Van Dorsselaer and Lapoujade. The calculated shapes for this paper

are both longer and have larger diameters. The calculated diameters are particularly exaggerated such that the calculated aspect ratio of length/diameter is 0.8 versus 1.1 in the experiment. Another difficulty with the present calculation is that the length of the EFP shape increases as long as the calculation is continued. The length, and to lesser extent the diameter, never stabilize to a constant value after reaching peak velocity.

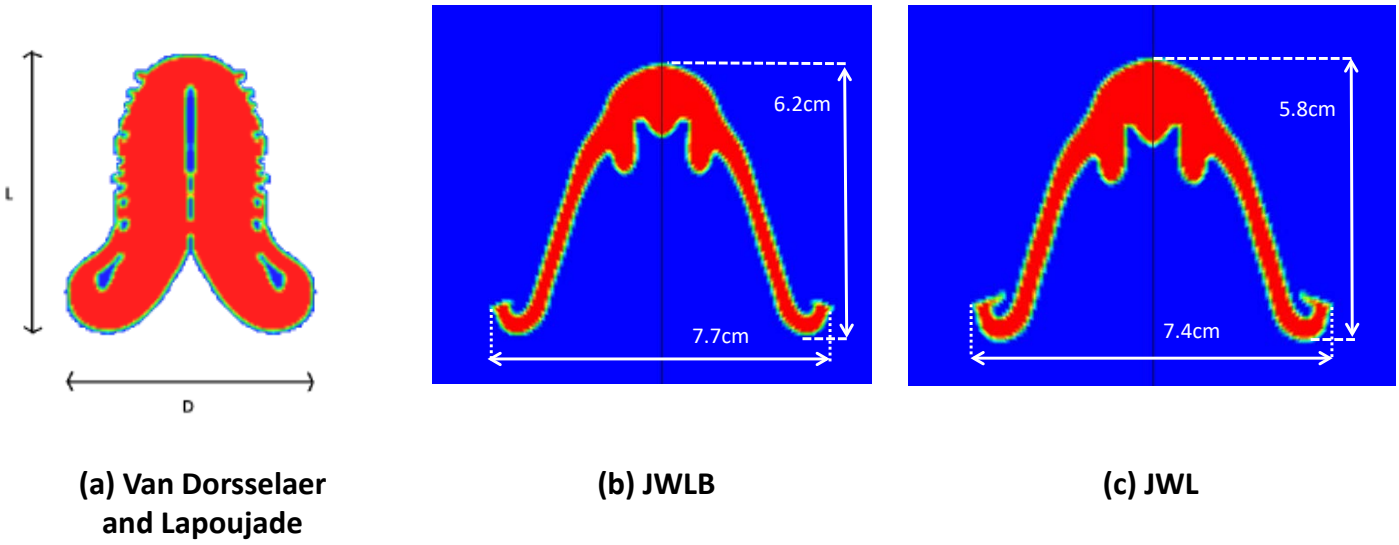

(a) Van Dorsselaer and Lapoujade **(b) JWLB** **(c) JWL**

Figure 3. EFP Shape Results [10]

Table 5. EFP Shape – Calculation vs. Experiment

Case	Length [cm]	Diameter [cm]	Length/ Diameter
Experiment	5.5	5.0	1.1
JWLB	6.2	7.7	0.8
JWL	5.8	7.4	0.8

In contrast to the results shown in Figure 3 and Table 5, calculation of the EFP shape reported by Van Dorsselaer and Lapoujade [10] using LS-DYNA agrees with the Hertel experiment. They used *MAT_JOHNSON_COOK as the constitutive model for the metals. Van Dorsselaer and Lapoujade report the % error results shown in Table 6 [10]; the results from the present calculations are included for comparison. V is peak velocity, D is diameter and L is length of the EFP. The shape of Van Dorsselaer and Lapoujade's EFP versus time is compared to the JWLB calculation in Figure 4.

Table 6. % Error between Simulations and Experiments – Van Dorsselaer and Lapoujade using CTH and LS-DYNA and LS-DYNA with JWLB EOS [10]

Parameter	% Error DL CTH	% Error DL LS-DYNA	% Error JWLB LS-DYNA	% Error JWL LS-DYNA
V	8.1	0.9	0.0	1.3
D	3.1	5.1	54.0	48.0
L	3.8	4.8	12.7	5.4

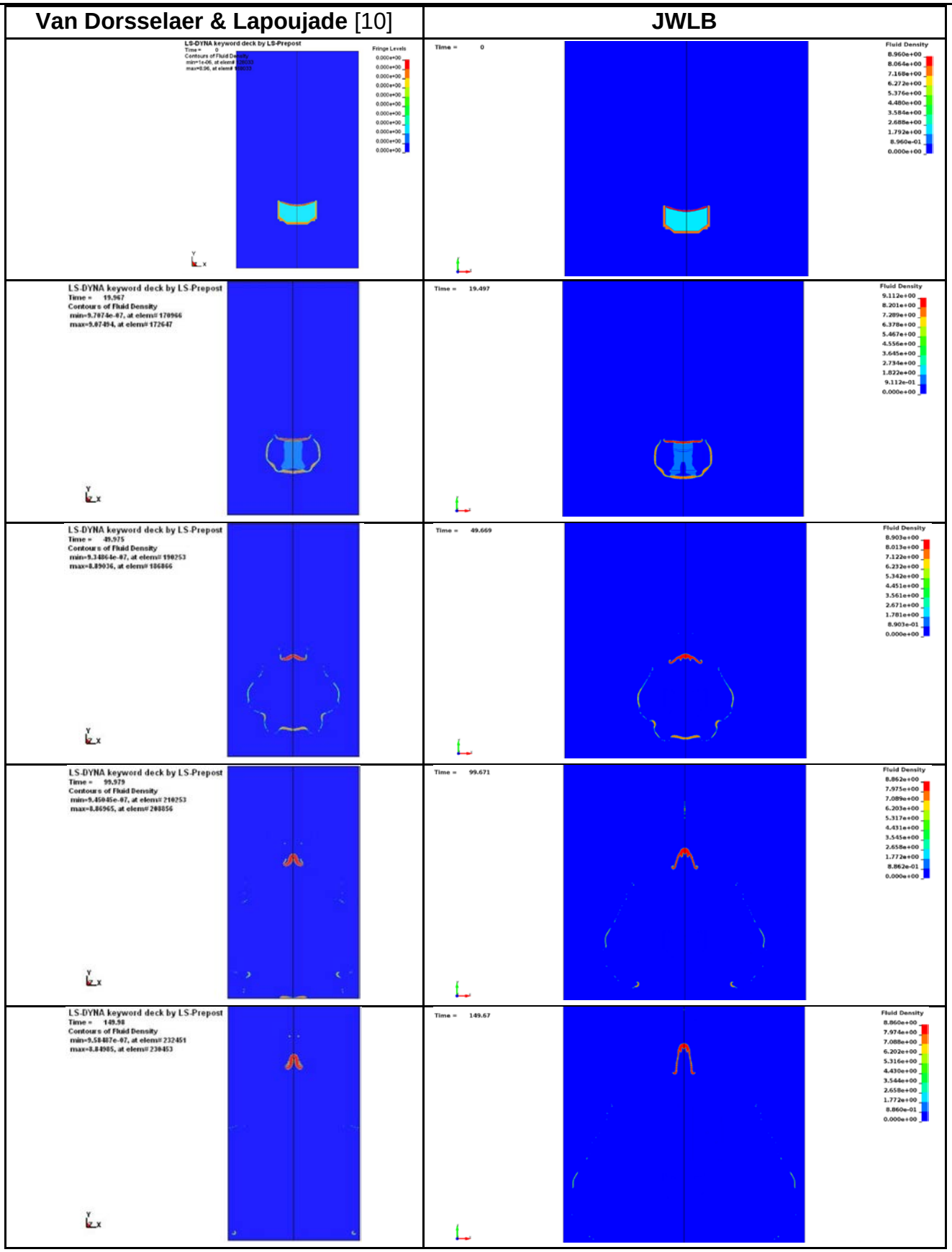

Figure 4. Shape – Fluid Density [g/cm³] vs. Time [usec]

Inconsistent EFP Shape – Possible Causes

Possible causes of the inconsistencies between the EFP shape from the present calculation, the Van Dorsselaer and Lapoujade calculation and the experiment were investigated. The details of the inputs used by Van Dorsselaer and Lapoujade were not available. Accordingly, the sensitivities of the calculated EFP shape to the following conditions were examined:

1. Element size and formulation
2. Initial geometry of casing, explosive and copper plate
3. Explosive equation of state
4. Copper plate
    a. Constitutive model
    b. Rate effects formulation for copper
    c. Failure model
5. Axisymmetric element formulation

Element Size

The results for peak velocity and shape discussed above for the present calculations were performed with 0.7mm square 2D shells for the Eulerian domain. Refining to a 0.35mm changed the initial velocity 5%, and, the EFP shape was not significantly different from the 0.7mm case. It is noted that the calculation with the 0.35mm mesh was less stable than with the 0.7mm mesh and crashed before reaching the termination time of the 0.7mm calculation.

Initial Geometry

Differences in the early-time shape of the EFP suggested that possible differences in initial geometries caused the inconsistent EFP shapes. As shown in Figure 4, the shapes of the EFP are already inconsistent at 20 usec. It was postulated that a difference in overpressure distribution at the explosive-casing junction caused the shape differences. The difference in overpressure distribution, in turn, was caused by differences in the geometry of the explosive-casing junction. Only a screen capture from the Hertel paper was available for developing the fill geometry for the present calculations, and imprecision in the fill geometry may have been a factor in the disagreement.

Accordingly, the sensitivity of the EFP shape to fill geometries was assessed. Calculations were performed where explosive was in the gap between the end of the copper plate and the casing. Other calculations were done where the end of the copper plate was placed in contact with the casing. Varying the fill geometry within these bounds did not significantly affect the EFP shape indicating the shape appeared insensitive to fill geometry.

Explosive Equation of State

As noted above, options for modeling the LX-14 with an EOS other than JWL were limited to JWLB. Input constants could not be obtained for IGNIITION_AND_GROWTH_OF_REACTION_IN_HE and JWL_AFTERBURN. Little difference was observed between the peak velocity and EFP shape, regardless of whether JWL or JWLB was used.

Copper Constitutive Model

Material 015 *MAT_JOHNSON_COOK has been observed to exhibit excessive softness. To check this possibility at a static loading rate, a coupon test was performed using *MAT_JOHNSON_COOK with inputs for copper [2], [3]. The stress and strain values output from the coupon test were consistent with values published in the *Atlas of Stress-Strain Curves* [11].

The calculation was run with the default log-linear Johnson-Cook rate effects for copper. Input constants for the log-linear form were from Johnson and Cook [2]. To assess sensitivity to rate effects form, Cowper-Symonds constants calculated from data published by Lindholm and Bessey [12] were used. This change in the rate effect formulation for the copper had negligible effect on the EFP shape.

Also, whether the Johnson-Cook failure parameters (D1 through D5) were included in the calculation did not significantly affect the EFP shape. More specifically, the calculation was run two ways: (1) no entries for D1 through D5 for the copper and (2) D1 through D5 for copper as reported in [3], with erode=1 such that there was no erosion. Rather, for erode $\neq 0$, deviatoric stresses are set to 0 upon failure. Again, difference in shape of the EFP was negligible.

Axisymmetric Element Formulation

Lastly, Benson has shown that volume-weighted axisymmetric element types underweight the nodes along the symmetry axis. The formulation is therefore not spherically symmetric [13]. This condition causes non-physical jetting along the axis of symmetry; the jetting is a byproduct of the element formulation, not caused by the physics of the calculation. Such jetting may explain the elongation of the EFP observed in the present calculations. However, Elform 14, which was used for the calculations, is an area-weighted formulation, and area-weighted formulations are known to preserve spherical symmetry [13]. As a result, it is uncertain whether the element formulation could be a contributing factor to the error in the EFP shape.

Conclusions

The 2D axisymmetric ALE finite element implementation accurately calculates the peak velocity of the copper EFP. The calculated peak velocity was within 2% of the peak velocity measured by Hertel if JWL EOS is used. Use of the JWLB EOS gave a peak velocity identical to Hertel's, within the precision of the calculation.

The calculation of the EFP shape was less accurate. The shape of the EFP was elongated compared with the measured shape. In addition, plastic flow continued as long as the calculation was continued; i.e., the EFP shape of the plate did not reach a dynamic equilibrium.

The sensitivity of the EFP shape was checked for these conditions: Eulerian domain element size and formulation; initial geometry of casing, explosive and copper plate; explosive equation of state and constitutive model for the copper plate. The shape was found to be insensitive to these conditions, when they were varied within reasonable bounds.

The excessive deformation of the copper plate was unexpected because the Johnson-Cook constitutive model is validated for multi-material ALE, though not necessarily for 2D axisymmetric ALE. It is possible that Johnson-Cook exhibits such excessive softness specifically when used with 2D axisymmetric ALE.

Another possible source of the excessive softness is the Johnson-Cook constitutive model itself. A candidate explanation is that the plasticity algorithm in Johnson-Cook fails to converge for the tolerance implemented in the LS-DYNA solver. Accordingly, plastic flow simply continues, independently of convergence.

A limited treatment of rate effects in the Johnson-Cook constitutive model may also contribute to the error. It is known that strain rate effects in steels are function of deformation. UFC 3-340-01 Figure 4-49 [14] has separate strength rate curves for yield and ultimate. Copper exhibits similar behavior, as discussed in Lindholm and Bessey [12].The copper plate undergoes large deformations, and it is likely that rate effects vary over those deformations, a property not included in the Johnson-Cook constitutive model.

It is observed in Lindholm and Bessey [12] that strength rate effects depend on temperature, but this effect is not explicitly included in the Johnson-Cook constitutive model.

Acknowledgements

The authors was would like to express appreciation to Len Schwer and Mhamed Souli for their observations and suggestions for improving the calculation. Nicolas Aquelet and Ian Do of LSTC generously reviewed the inputs and results of the calculations and provided comments. Finally, the authors thank Sam Rigby of the University of Sheffield and Ernie Baker of Munitions Safety Information Analysis Center (MSIAC) for reviewing the paper and providing helpful comments.

References

[1] E. S. Hertel, "SAND-92-1879 A Comparison of the CTH Hydrodynamics Code with Experimental Data," Sandia National Laboratories, Albuquerque, NM, 1992.

[2] G. R. Johnson and W. H. Cook, "A Constitutive Model and Data for Metals Subjected to Large Strains, High Strain Rates and High Temperatures," Contract F08635-81-C-0179 U.S. Air Force and Honeywell Independent Development Program.

[3] G. R. Johnson and W. H. Cook, "Fracture Characteristics of Three Metals Subjected to Various Strains, Strain Rates, Temperatures and Pressures," *Engineering Fracture Mechanics*, vol. 21, no. 1, pp. 31-48, 1985.

[4] "LS-DYNA Keyword User's Manual: Volume II Material Models," Livermore Software Technology Corporation, Livermore, CA, 2017.

[5] D. Steinberg, "Equation of State and Strength Properties of Selected Materials," Lawrence Livermore National Laboratory, Livermore, CA, 1996.

[6] M. Otsuka, Y. Matsui, K. Murata, Y. Kato and S. Itoh, "A Study on Shock Wave Propagation Process in the Smooth Blasting Technique," Livermore Software Technology Corporation, Livermore, CA, 2004.

[7] B. Fuller, S. Rigby, A. Tyas, S. Clarke, J. Warren, J. Reay, M. Gant and I. Elgy, "Experimentation and Modeling of Near Field Explosions," in *Military Aspects of Blast and Shock*, Halifax, NS, Canada, 2016.

[8] E. L. Baker, R. E. Cornell and L. I. Stiel, "Understanding Experimental and Computation Gurney Energies," in *U.S. Army ARDEC*, Picatinny, NJ.

[9] C. Tarver, Lawrence Livermore National Laboratory, Livermore, CA: Email Correspondence, 9 June 2017.

[10] N. Van Dorsselaer and V. Lapoujade, "A Contribution to New ALE 2D Method Validation," in *11th International LS-DYNA Users Conference*, Dearborn, MI, 2010.

[11] Atlas of Stress-Strain Curves, Materials Park, OH: ASM International, 2002.

[12] U. S. Lindholm and R. L. Bessey, "AFML-TR-69-119 A Survey of Rate Dependent Strength Properties of Metals," Air Force Material Laboratory, Wright-Patterson Air Force Base, OH, Apil 1969.

[13] D. J. Benson, Computational Methods in Lagrangian and Eulerian Hydrocodes, La Jolla, CA: University of California, San Diego, 1990.

[14] "UFC 3-340-01 Design and Analysis of Hardened Structures to Conventional Weapons," U.S. Department of Defense, Washington, DC, 2002.